J Physiol Sci (2012) 62:133–145
DOI 10.1007/s12576-011-0191-6

ORIGINAL PAPER

Vascular tortuosity: a mathematical modeling perspective

Leith Hathout · Huy M. Do

Received: 27 October 2011 / Accepted: 30 December 2011 / Published online: 18 January 2012

Abstract Although vascular tortuosity is a ubiquitous phenomenon, almost no mathematical models exist to describe its shape. Given that the shape of tortuous vessel curves seems fairly uniform across orders of magnitude of vessel size and across vast differences in anatomic substrata, it is hypothesized that the shape of tortuosity is not purely random but rather is governed by physical principles. We present a mathematical model of tortuosity based on optimality principles, and show how this model can potentially be used to distinguish physiologic tortuosity from abnormal tortuosity which may exist in disease states. Using the calculus of variations, a model of tortuosity has been developed which minimizes average curvature per unit length. The model is tested against curves in normal vessels and in diseased vessels in a case of Fabry's disease. It is found that the theoretical model provides a good fit for normal vessel tortuosity. This suggests that blood vessels obey optimality principles, and curve in such a way as to minimize average curvature. The model may also be able to distinguish physiologic tortuosity from abnormal tortuosity found in disease states.

Keywords Mathematical modeling · Vascular tortuosity · Optimality analysis

Introduction

As every angiographer knows from experience, blood vessels are often tortuous. This can make threading a catheter into such a vessel challenging. However, the phenomenon of vessel tortuosity is interesting and important in its own right, beyond the difficulties it may pose during an angiogram. This is because the phenomenon seems ubiquitous to blood vessels throughout the body, from small vessels in the retina of the eye to larger vessels such as mesenteric and splanchnic vessels, the cervical carotid arteries and their branches, the cerebral vasculature, the superficial temporal artery and the coronary arteries (Fig. 1).

Moreover, the general meandering shape of the tortuosity often seems fairly uniform across multiple vessels and across different individuals, regardless of the markedly varying anatomic structures within which these vessels are coursing. This general uniformity suggests that the phenomenon of tortuosity is not purely random or accidental but rather is governed by certain physical principles which bring about a similar shape to the vessel curves across great variations in vessel size and great differences in anatomic substrata. The aim of this paper is to test this assumption by exploring a mathematical model of vessel tortuosity which attempts to describe the shapes associated with tortuosity and to uncover some of the underlying principles which govern those shapes, and then to test this model against actual vessel data. Such a model, of necessity, will be an oversimplification because of the almost infinite variety of anatomical structures which force vessels to curve this way and that. However, since this phenomenon has not been systematically modeled in the literature, it is useful to begin an investigation which can later be augmented and complexified. This is particularly true given emerging data which suggests that the phenomenon of normal tortuosity may be disturbed in multiple disease states.

Indeed, in recent years, several papers have appeared suggesting that the assessment of vascular tortuosity may

L. Hathout (✉)
Department of Biology, Stanford University, Palo Alto, USA
e-mail: lhathout@stanford.edu

H. M. Do
Department of Radiology, Stanford University Medical Center, Palo Alto, USA

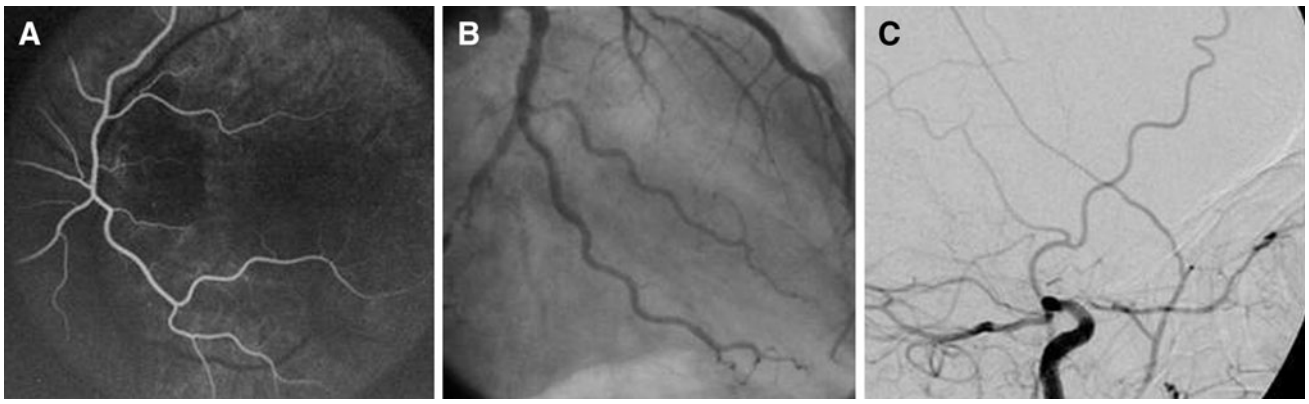

Fig. 1 **a** Normal retinal fluorescein angiogram showing multiple tortuous vessels [1]. **b** Coronary angiogram showing tortuous coronary artery branches. **c** Cerebral angiogram showing a tortuous superficial temporal artery

be clinically significant in a variety of settings. Malamateniou et al. [2] found statistically significant decreased tortuosity in all proximal segments of the cerebral vasculature (anterior, middle and posterior cerebral arteries) in preterm infants imaged at term-equivalent age compared to the term-born infants. Since brain development is closely linked to vascular development, the possibility is raised that this phenotype may correlate with later neurodevelopmental dysfunction in preterm infants [3]. Conversely, in the healthy elderly, Bullit et al. [4] have noted that increased aerobic activity is associated with lower cerebral vessel tortuosity values and an increase in the number of small-caliber vessels. They hypothesize that this may be part of the link between aerobic exercise and healthy brain aging [4]. Witt et al. [5] have noted that decreased retinal vascular tortuosity was predictive of an increased risk of death from ischemic heart disease.

Most significant, though, are the applications of tortuosity analysis in cancer. Bullit et al. [6] have done a significant body of work showing that malignant tumors display abnormal and increased vessel tortuosity. This finding is highly significant in that it represents an independent measure of tumor angiogenesis separate from perfusion measurements, which may remain normal despite the presence of abnormal tortuosity. Preliminary work by this same group suggests that early tumor detection, prediction of tumor response to therapy, and detection of tumor recurrence are all linked to increased abnormal vessel tortuosity [7–10]. Jain also notes that tumor vessels show increased vessel length, density, and tortuosity, and suggests that normalizing tumor vascularity may be an important adjunct to tumor therapy [11].

Given these new avenues of research, it becomes important to explore models of normal vessel tortuosity. The model used in this paper was originally developed in the field of geophysics in the 1960s to analyze the meandering of rivers. To the best of the authors' knowledge, this paper represents the first attempt to apply such models to the phenomenon of vascular tortuosity. The model is used to obtain a family of equations approximating the shape of vessel curves. Specific parameters are extracted which characterize the shape of normal tortuosity. Using these parameters, the model is then tested against normal vessel segments to assess its accuracy in describing the shape of vessel curves. Finally, albeit anecdotally, vessel segments from a clinical case with known abnormal vascular tortuosity are analyzed to assess whether the model can detect and quantify deviations from normal tortuosity. This is done only as an illustration of method. Further work, of course, will be necessary to validate and refine this initial model, as well as to test its utility in disease states.

Materials and methods

Mathematical modeling

Since mathematical modeling is undertaken with an eye to comparing some model-generated parameters with the results from actual vessels, this requires the extraction of convenient physical parameters which characterize the shape and degree of tortuosity. In this paper, we will adopt the convention used in geophysics in the analysis of river meanders [12]. The main parameters of interest of a curve will be the path length (called L) of a particle or blood cell flowing along the curved segment, the wavelength λ, defined as in a cosine or sine wave as distance from trough to trough or point of inflection to point inflection, and the radius of curvature R, which defines the radius of a circle which has as its arc the peak of the curve. To normalize for the effect of vessel length, and give dimensionless numbers

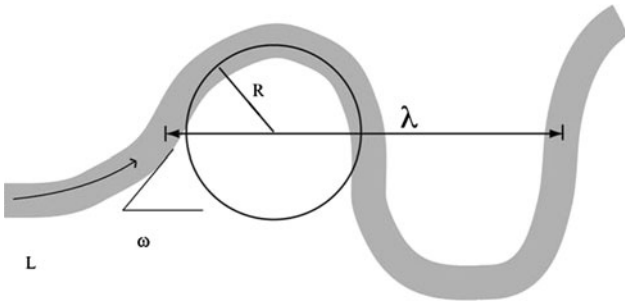

Fig. 2 The parameters of interest in analyzing tortuosity. L is path length, λ wavelength, and R radius of curvature. The maximal direction angle is ω. This is considered as a given in the model—it may be the result of chance, or local anatomy

which can be compared between vessels and the model, these parameters are combined into two ratios, L/R, and L/λ, which characterize a vessel's curvature. The latter ratio, L/λ, is known as the sinuosity of a curve. An additional parameter of interest is ω, the maximal angle which the curve of the vessel makes with the "horizontal," which in the case of vessels is defined as the direction of vessel flow (see Fig. 2).

For the purposes of this preliminary investigation, we chose to model vessel tortuosity by finding an approximation to the curve which has the least average curvature per unit length. In other words, the curve which, as it meanders between two points, A and B, provides the minimum changes in direction for the blood flowing through the tortuous vessel. Of course, the absolute minimum change in direction would be a straight line segment between points A and B, a course to which blood vessels often adhere. We assume that when vessels deviate from this straight-line course, this may be due to an anatomic obstacle, or to a random change in direction, which begins the vessel on a meandering path. The question is then to specify the shape of this path according to the optimality criterion presented above.

The derivation of the differential equation which specifies the desired curve is fully presented in Appendix A. Briefly, assume that the curve has total length L. For any point $P(x,y)$ on this curve, if l is the path length to travel to this point along the curve, then we let functions $x(l)$ and $y(l)$ describe the position of a point on the curve and $\theta(l)$ describe the direction of the curve at that point. Under these assumptions, the curve can be specified parametrically as a function of the direction angle $\theta(l)$ as

$$x(t) = \int_0^t \cos\theta\,(l)\,\mathrm{d}l \quad y(t) = \int_0^t \sin\theta\,(l)\,\mathrm{d}l$$

where t is a variable parameter in the segment $(0, L)$.

We can define the average curvature, $\bar{c}$, as the integral square average of $\theta'(l)$ (see Appendix A):

$$\bar{c} = \sqrt{\frac{1}{L}\int_0^L (\theta'(l))^2\,\mathrm{d}l} \tag{1}$$

This is the continuous analog of the mean square value of n numbers.

Our interest is to find the curve that has the minimum average curvature, assuming a curved path.

This problem can be specified using the technique of Lagrange multipliers, to yield the integral

$$\int_0^L (\theta'(l))^2 + \lambda\left(\cos\theta\,(l) - \frac{X_1}{L}\right) + \mu\left(\sin\theta\,(l) - \frac{Y_1}{L}\right)\mathrm{d}l$$

where

$$X_1 = x\,(L) = \int_0^L \cos\theta\,(l)\mathrm{d}l$$

$$Y_1 = y\,(L) = \int_0^L \sin\theta\,(l)\mathrm{d}l$$

We are now searching for the function $\theta(l)$ which minimizes the above integral.

This problem can be solved using standard techniques of the calculus of variations, e.g., the Euler–Lagrange equation and Lagrange multipliers (see Appendix B).

It is found that the required function satisfies the following differential equation:

$$\frac{\mathrm{d}\theta}{\mathrm{d}l} = \alpha\sqrt{\cos\theta - \cos\omega}$$

The solution of this differential equation is a so-called elliptic integral, which cannot be written in closed form. However, it can be approximated by the following equation which provides a tractable form for $\theta(l)$ (see Appendix B):

$$\theta(l) = \omega\sin\left(\frac{2\pi l}{L}\right) \tag{2}$$

This curve, known as a "sine-generated" curve, is characterized by ω, the maximal angle it makes with the horizontal.

The average curvature per unit length, as defined above, can now be rewritten as:

$$\bar{c} = \sqrt{\frac{1}{L}\int_0^L (\theta'(l))^2\,\mathrm{d}l} = \sqrt{\frac{1}{L}\int_0^L \frac{4\pi^2\omega^2\left[\cos\left(\frac{2\pi l}{L}\right)\right]^2}{L^2}\,\mathrm{d}l}$$

The radius of curvature, R, of the sine-generated curve at its peak (as shown in Fig. 2) can also be theoretically

calculated. The answer comes out in very simple form: $R = \frac{L}{2\pi\omega}$. In comparing the results of the model to vessel data, we are interested in the ratio L/R (to normalize by vessel length). This has the even simpler form:

$$L/R = 2\omega\pi. \quad (3)$$

Not discussed further in this paper are a variety of checks we performed against normalized sine curves and spline curves to verify that the sine-generated curves given by Eq. 2 indeed provide the curves of minimum average curvature as defined by Eq. 1.

Blood vessel measurements

The mathematical parameters of interest, L/R, and L/λ, can all be measured on vessel segments for comparison to the mathematical model (Fig. 3). For the model and the measurements on vessels, the wavelength is defined as in a sine/cosine wave, from trough to trough.

Thirty-four vessel segments were chosen from sequential angiograms performed at our hospital, including coronary, superficial temporal, retinal, hepatic, renal, gastric, splenic, and mesenteric arteries. Patient ages ranged from

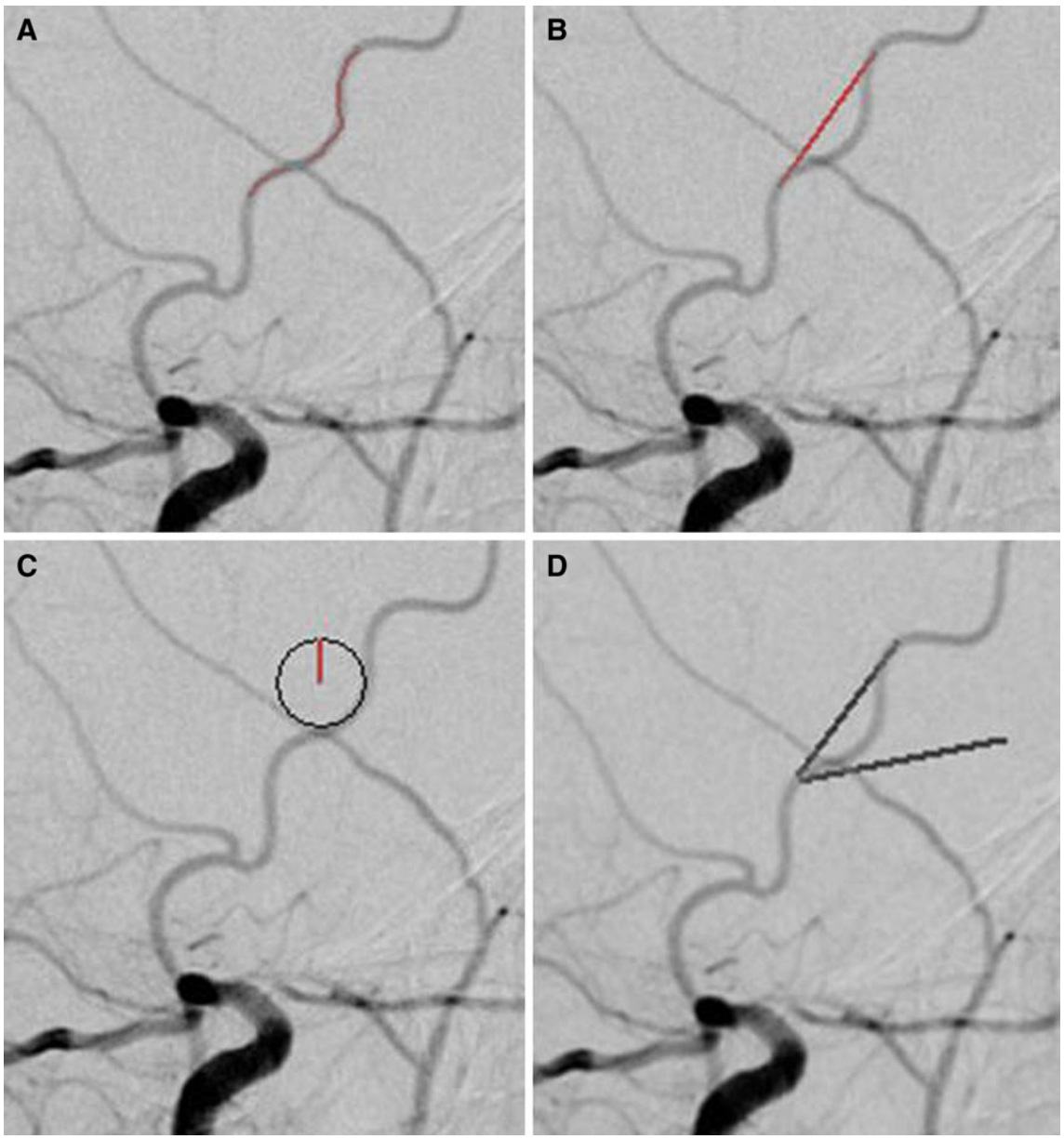

Fig. 3 Angiographic images illustrating the measurement of path length L (**a**), wavelength λ (**b**), radius of curvature R (**c**), and maximal direction angle ω (**d**) on a vessel segment in the superficial temporal artery

19 to 97, with an average age of 59. Patients with coronary angiograms were being worked up for angina and valvular disease (mitral regurgitation). Abdominal angiograms were performed primarily for hepatocellular carcinomas. Cerebral angiographic studies were performed for patients with headache, CVA, and TIA, and one patient with moya moya. In all cases, normal vessels were chosen away from the region of disease (e.g., splenic, renal, or mesenteric arteries from angiograms performed for hepatocellular carcinoma).

Using Universal Ruler, the wavelength λ, path length L, radius of curvature R, and maximal angle of deflection from the flow direction ω, were manually measured and tabulated as shown in Fig. 3. For each vessel segment, the ratios L/R, and L/λ were calculated. For each vessel segment, these values were then compared to the theoretical values obtained from the corresponding sine-generated curve (determined by the same value of ω).

Results

Results of the mathematical model

Using the techniques of the calculus of variations (see "Mathematical modeling", above, and Appendices A and B), a closed form mathematical function is derived which provides a curve of minimum average curvature per unit length. This is called a sine-generated curve (Eq. 2), whose intrinsic form, $\theta(l) = \omega \sin\left(\frac{2\pi l}{L}\right)$, represents an infinite family of curves, each specified by the value of ω. Any curve of this family can be transformed into a set of parametric equations which represent the curve conventionally on Cartesian coordinates:

$$x(t) = \int_0^t \cos(\phi(l))\,\mathrm{d}l = \int_0^t \cos\left[\omega \sin\left(\frac{2\pi l}{L}\right)\right]\mathrm{d}l$$

$$y(t) = \int_0^t \sin(\phi(l))\,\mathrm{d}l = \int_0^t \sin\left[\omega \sin\left(\frac{2\pi l}{L}\right)\right]\mathrm{d}l$$

The shape of the sine-generated curve will be essentially uniquely determined by ω. Figure 4 shows the appearance of the sine-generated curves for several values of ω. It is noted that sinuosity (the ratio L/λ) increases with increasing ω.

It is stressed that the sine-generated curve is not a sine (or cosine) curve. The curve itself is not sinusoidal. Rather, its direction angle varies in a sinusoidal fashion with distance along the curve. This is illustrated in Fig. 5.

Parameters of interest for the sine-generated curves are the ratio of the path length L to the wavelength λ, and the ratio of L to R. These parameters are calculated using Matlab. L/R is given directly by Eq. 3 ($L/R = 2\omega\pi$), while $s = L/\lambda$ is easily obtained as part of the Matlab programming of the curves.

As can be seen from Fig. 4, both L/R and sinuosity, $s = (L/\lambda)$, vary directly with ω. For smaller values of ω, the curve is less steep, and hence the radius of curvature is bigger. Thus, both L/λ and L/R are smaller for smaller ω.

Since vessels appear sinusoidal, some may assume that they can be described by simple sine curves. To test the standard sine curve for goodness of fit against the sine-generated curve in comparison to real vessel data, both L/R and sinuosity (L/λ), need to be obtained for the sine curve. This can be done by integration using the following formulas from calculus, and recalling that for the sine curve, $\lambda = 2\pi$:

$$y = \sin x$$

$$L = \int_0^{2\pi} \sqrt{1 + \left(\frac{\mathrm{d}y}{\mathrm{d}x}\right)^2}$$

$$R(x) = \frac{\left[1 + \left(\frac{\mathrm{d}y}{\mathrm{d}x}\right)^2\right]^{3/2}}{\frac{\mathrm{d}^2 y}{\mathrm{d}x^2}}$$

The radius of curvature, R, is calculated at the peak of the sine curve, i.e. $x = \pi/2$. Using these formulas, we get for the sine curve that sinuosity $(L/\lambda) = 1.216$, and $L/R = 7.64$.

Results of vessel analysis

As shown in Fig. 3, the same parameters that were calculated for the sine-generated curves can be measured for actual vessel segments. Analysis of the tortuous segment of superficial temporal artery shown in Fig. 3 yields the following results: the measured value of ω is 42°. The corresponding sine-generated curve with an ω of 42° has an L/λ of 1.14 and an L/R of 4.61. For the actual vessel, measured values in pixel units are $L = 78$, $\lambda = 68$, and $R = 16$, leading to calculated values of $L/\lambda = 1.15$ and $L/R = 4.88$. This corresponds to absolute value errors of 0.62% in L/λ and 5.44% in L/R.

In Fig. 6, the same analysis is undertaken for a left coronary artery segment. The measured value of ω is 24°. The corresponding sine-generated curve with an ω of 24° has an L/λ of 1.05 and an L/R of 2.64. For the actual vessel, measured values in pixel units are $L = 339$, $\lambda = 311$, and $R = 130$, leading to calculated values of $L/\lambda = 1.09$ and $L/R = 2.61$. This corresponds to absolute value errors of 3.67% in L/λ and 1.24% in L/R.

As can be seen from the above examples, a direct comparison can be made between measurements on tortuous vessel segments and theoretical results from the

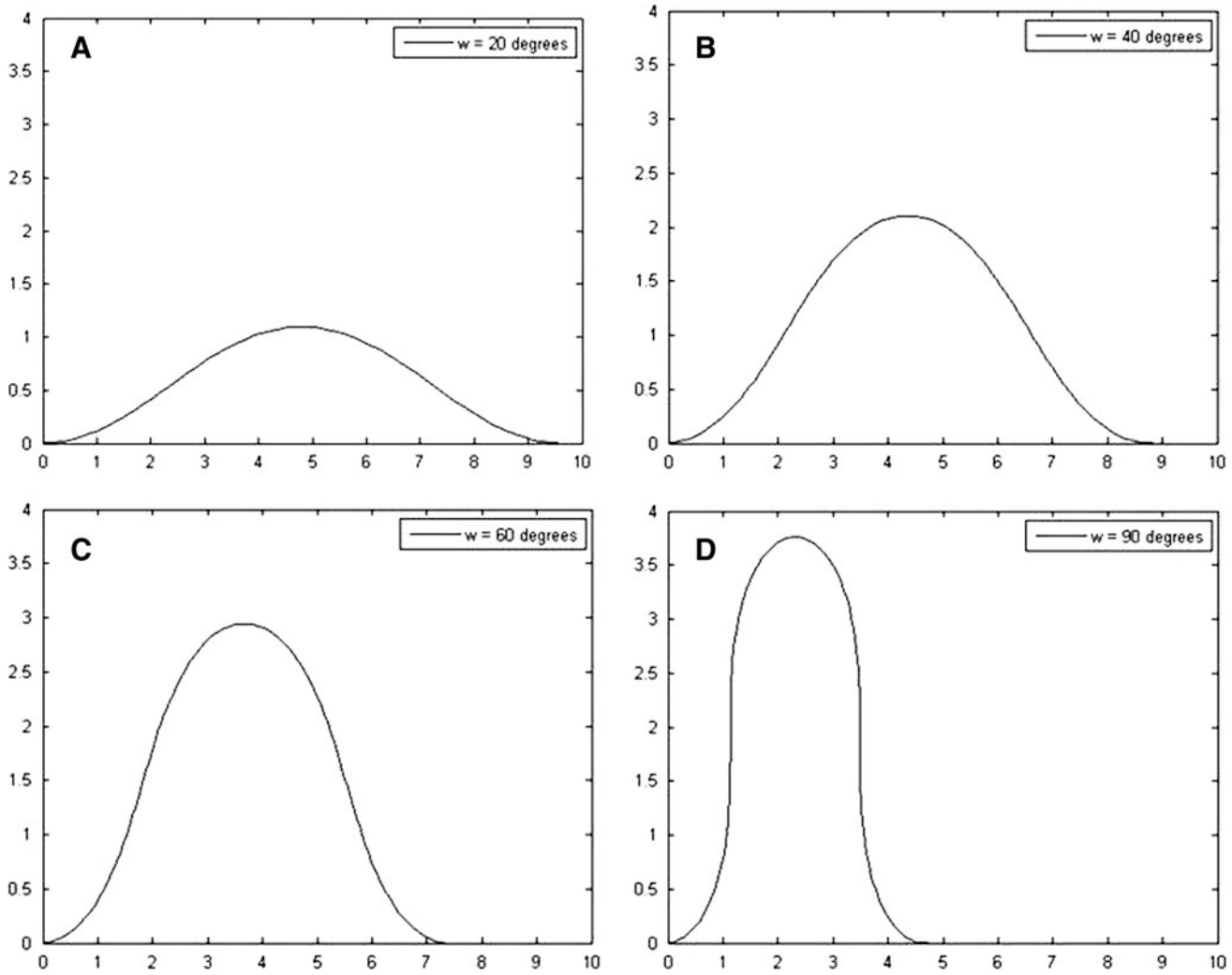

Fig. 4 Sine-generated curves for $\omega = 20$ (**a**), 40 (**b**), 60 (**c**) and 90 (**d**). These curves are rendered in Matlab using numerical integration, assuming a path length (L) of 10 and a step length of 0.1. It is noted that sinuosity (the ratio L/λ) increases with increasing ω

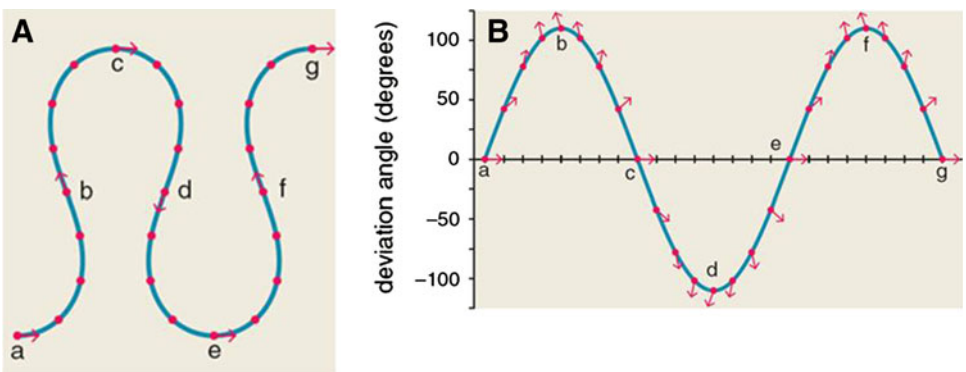

Fig. 5 **a** Sine-generated curve for $\omega = 110°$. Points are specified along the curve where the direction angle φ is measured. **b** A graph of the direction angle as a function of distance along the sine-generated curve in **a**. Modified from original with the kind permission of Brian Hayes and *American Scientist*

corresponding sine-generated curves, as determined by the appropriate value of ω, the maximal angle which the vessel makes with the "horizontal", i.e., the direction of vessel flow.

For all vessel segments, compared to their corresponding sine-generated curves, the average absolute value percent error for L/λ is 5.53 ± 4.1%, and the average absolute value percent error for L/R is 5.83 ± 4.3%.

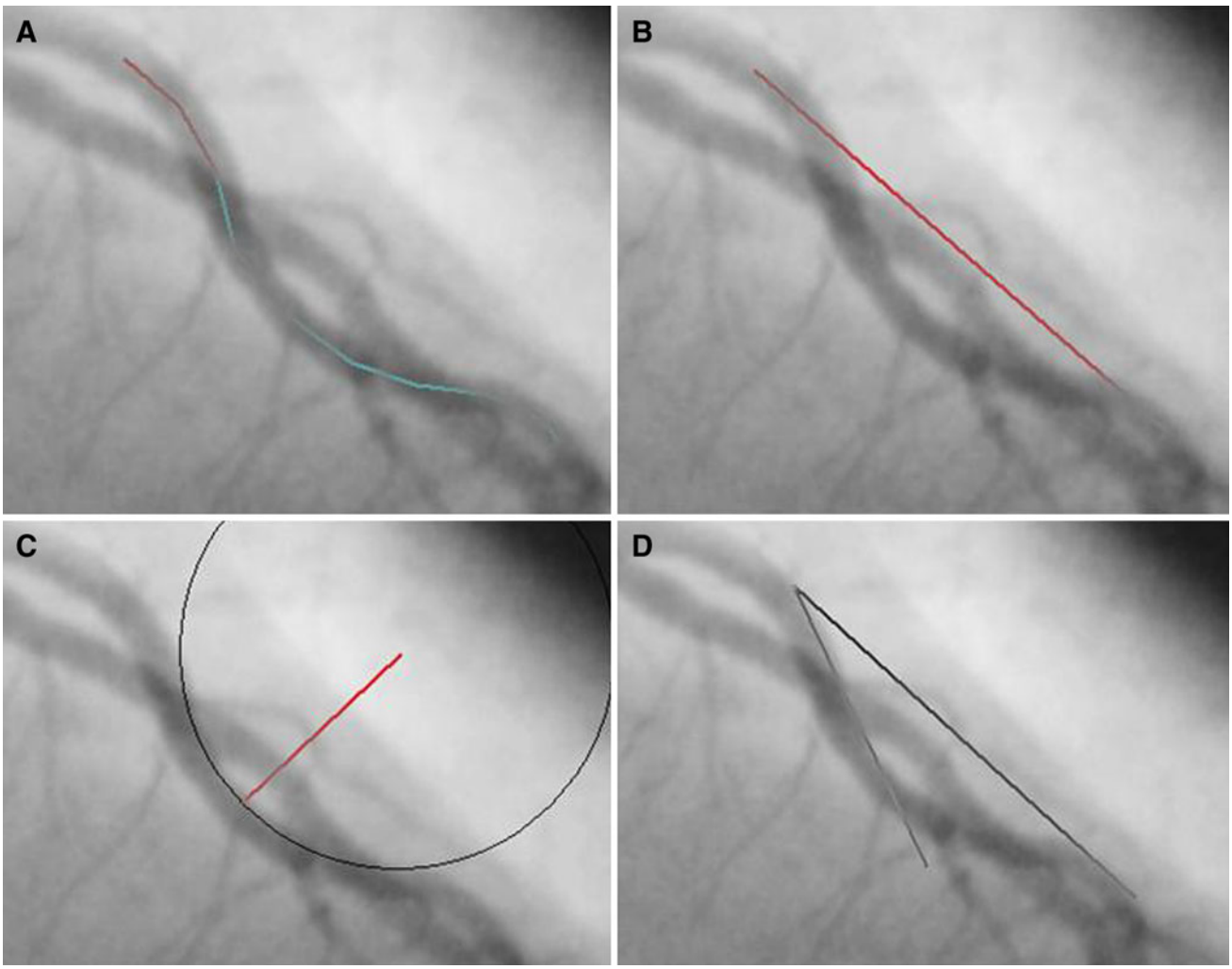

Fig. 6 a–d Tortuous segment of a left coronary artery. ω is measured at 24°. Based on this, the theoretical value of L/λ is 1.05 and of L/R is 2.64. For the vessel segment, calculated values of L/λ are 1.09 and of L/R are 2.61. This corresponds to absolute value errors of 3.67% in L/λ and 1.05% in L/R

When the vessel data are compared to a standard sine wave, the average absolute value percent error for L/λ is $12 \pm 11.6\%$, while for L/R, it is $52.8 \pm 53\%$.

A Student's t test for samples with unequal variance shows that, in comparison to actual vessel data, the sine-generated curve gives a better fit than a sine curve with high statistical significance. For L/λ, $p = 0.001$, while for L/R, $p = 3.93 \times 10^{-6}$.

Discussion

The phenomenon of vascular tortuosity is so ubiquitous across the vascular tree, and the appearance of tortuosity is so similar across vessels of vastly different sizes and locations within the same individual, as well as across individuals at large, that the phenomenon does not appear to be random or accidental. Rather, these similarities suggest that there is some physical cause underlying and governing the shape of vessel curves.

Given the emerging clinical significance of the study of normal versus abnormal tortuosity, it becomes important to investigate whether valid mathematical models can be developed which reasonably describe the shape of blood vessels as they curve. If such models can be found, it not only opens the door to understanding why normal tortuosity has the shape it does (as an interesting physiological question) but also to investigating and quantifying the phenomenon of abnormal tortuosity. For example, as noted by Bullit et al. [7], "vessel shape analysis could provide an important means of assessing tumor activity". Such an analysis, however, would optimally require some understanding of the shape of the normal, or physiologic, tortuosity ubiquitously found in vessels. If such modeling

efforts are fruitful, then the analysis of vessel tortuosity could move from the binary realm of "increased" or "decreased" tortuosity, as is present in much of the current literature, to asking the additional question of "normal" versus "abnormal" tortuosity, as astutely posed by Bullit et al.

Thus, modeling would facilitate more accurately posing and answering such questions as whether disease states produce a type of tortuosity which deviates from normal, and perhaps quantifying, according to specific parameters derived from modeling, the degree of deviation from physiologic tortuosity. It is important to note that such deviations do not always imply increased tortuosity. As cited above, decreased retinal tortuosity may correlate with the increased risk of death from ischemic heart disease, while decreased cerebral vessel tortuosity is a phenotype associated with premature birth, and which does not recover when age is adjusted to term. Furthermore, Saba and Mallarini [13] have investigated the relationship of the tortuosity of cervical internal carotid arteries and the risk of stroke, finding that increased "coils," do not lead to greater stroke risk, but that increased "kinks" do increase the risk of ischemic stroke. Clearly, these qualitative findings imply that "more," or "less," tortuosity are insufficient descriptors, and that the shape of the tortuosity matters. Such analyses, including the important analysis of tumor vascularity, would thus be greatly enhanced by the availability of valid mathematical models of physiologic tortuosity, which describe the shape of the normal meandering of vessels.

A key question in building a model de novo is to specify the main physical principle or principles which are believed to govern the shape of normal tortuosity. It is, of course, understood that no single principle or set of principles will be sufficient to fully specify the shape of tortuosity, as in the human body there will be enormous complexities given the variability of anatomic structures, random physical variations, etc., which will influence vessel shape and course. Thus, the model is by necessity an idealization and simplification of the true course of blood vessels. However, given the significance of blood vessels to higher life forms, and the sheer enormity of the vascular network, it is assumed that such a system would obey some principles of optimal design. Such a notion is not entirely novel, and principles of optimality have been previously used to model the branching patterns within the vascular tree [14]. Such models relied on the notion of cost minimization, attempting to minimize the work done in pumping blood through a branching vascular network.

This paper models the phenomenon of physiologic tortuosity with the assumption that the underlying physical principles which govern the shape of tortuosity also obey constraints of optimality. Knowing that vessels curve, the model is based on finding the curved path of minimal average curvature between two points. In other words, the model gives the path for which the sum of the squares of changes in angular direction that a particle would make when traveling this path is minimized. In theory, this should minimize the shear stress against vessel walls caused by blood having to change direction. Also, it should help minimize the energy needed to accelerate blood through the vessel.

Our analysis is based on prior studies of tortuosity in nature, which formulated this model to analyze the phenomenon of meandering in flowing rivers, which somewhat resembles the tortuosity of vessels. While the original derivations of Leopold, Langbein and Luna [15] used a probabilistic analysis to derive the sine-generated curves, this paper presents the river meandering analysis of Movshovitz-Hadar and Shmukler (see Appendices A and B for their derivation), setting up the optimization problem as a deterministic problem in the calculus of variations, and solving the resulting differential equation [16].

The model shows that the optimal curve in terms of minimizing average curvature per unit length can be closely approximated by a function known in mathematics as a "sine-generated" curve (Eq. 2). This belongs to a class of intrinsic functions which describe a curve by specifying its "direction angle," i.e., by describing how the direction of the curve changes in terms of the angle it makes with respect to the horizontal at each point along its path. For the sine-generated curve, the direction angle of the curve varies in a sinusoidal fashion along the length of the curve. Once again, it is important to stress that such a curve is not a sine curve, wherein the curve itself is sinusoidal. Rather, for a sine-generated curve, the direction angle of the curve, as a function of distance along the curve, varies in a sinusoidal fashion.

Having found this curve, we can see that if the sine-generated curve is a good approximation to the vessel shape, then there will be a good correspondence between the theoretical values of L/λ and L/R as calculated for the sine-generated curves and as measured for the vessels. If, on the other hand, the vessel tortuosity is of a significantly different shape than the sine-generated curve, there will be a significant discordance between these values.

Our results demonstrate that this curve, according to the parameters extracted from the model, provides a good description of vessel tortuosity, with average absolute value percent errors of 5–6%, and a significantly better fit than that provided by a standard sine curve. Given the almost infinite variety of the microstructures through which these vessels course, this is an excellent agreement, suggesting that a model such as this is a reasonable characterization of vessel tortuosity.

Interestingly, it is noted that a probabilistic approach to mathematical modeling leads to the same mathematical

model as the deterministic calculus of variations model we employed. If a particle takes a random walk from point A to point B in a fixed number of steps, while able to change its direction at random at each step, it is possible to search for the most probable resulting curve. This leads to the same result as the deterministic calculus of variations analysis [17]. Thus, the sine-generated curve derived by the model possesses simultaneously three remarkable properties which, on theoretical grounds, suggest that it may reflect nature's way of shaping blood vessel tortuosity:

1. It is the curve with the minimum average curvature as described above.
2. It is the curve of minimal total work in bending (because the sum of the squares of changes in direction is minimized). Thus, if an elastic rod is bent by pushing its two ends together, the shape of the resulting curve will be nearly identical to the sine generated curve [18].
3. It is the curve which represents the average, or most probable path, taken by a random walk of fixed length [17]. Thus, if we assume that vessels, as they are budding or coursing through tissue, are choosing their direction randomly at each infinitesimal increment of length, constrained to start at point A and end at point B, the resulting "average" path will lead to the same equations which produced the sine-generated curve deterministically.

These results are important in seeking an understanding of the phenomenon of physiologic tortuosity. More important, though, is the potential impact of this sort of modeling in the study of how tortuosity can deviate from normal in disease states, particularly in tumors. Understanding the shape of physiologic tortuosity can provide a framework to identify and quantify deviations from normal.

Although entirely anecdotal, this approach is tested on 6 retinal vessel segments from a case of Fabry's disease [19], known to cause abnormal vascular tortuosity (see Fig. 7 and compare with Fig. 1a). In these vessel segments, there is a significant deviation from the parameters calculated for the corresponding sine-generated curves, with absolute value average percent errors of 21.4% in L/λ and 33.2% in L/R. This indicates that these vessels deviate from the normal or physiologic pattern of tortuosity (i.e., do not follow the shape of sine-generated curves). This retinal angiogram was obtained as part of depersonalized data submitted to the Fabry Outcome Survey (FOS), a European patient registry with the most comprehensive existing data base on Fabry patients [19]. From this database, it is known that retinal vessel tortuosity is present in 48.7% of male patients, with this finding presenting at an average age of 31.9 ± 13.1 years [20]. Fabry's disease is an X-linked lipid storage disease secondary to deficiency of the enzyme alpha galactosidase A; thus, it has broad systemic manifestations, most notably with cardiac, renal, ocular, and neurologic abnormalities. The most common ocular manifestation is cornea verticillata, reported in 73.1% of male patients [21]. However, this finding was not found to correlate either with disease severity or the likelihood of disease progression. The presence of retinal vascular tortuosity, conversely, was found to be strongly correlated both with disease severity at presentation ($p = 0.01$), as well as with disease progression [21]. For example, patients with retinal vessel tortuosity showed a more progressive deterioration of renal function ($p = 0.01$) and a more rapid increase in cardiac size ($p < 0.01$) [21]. Furthermore, the mean age at presentation of left ventricular hypertrophy was 39.4 years, and for renal disease requiring dialysis was 39.6 years, i.e., approximately 8 years after the detection of retinal vascular tortuosity [20], suggesting that the detection of retinal vascular tortuosity has prognostic significance. This conclusion was reached by the FOS investigators, who stated that the FOS data "suggest a positive predictive value in performing regular eye examinations (particularly focusing on vessel tortuosity) in patients with systemic involvement". [21]. Thus, this case, while only illustrative of method, along with the FOS data, underscores the importance of detecting retinal vessel tortuosity, and provides an example of the potential utility of models such as the one presented here.

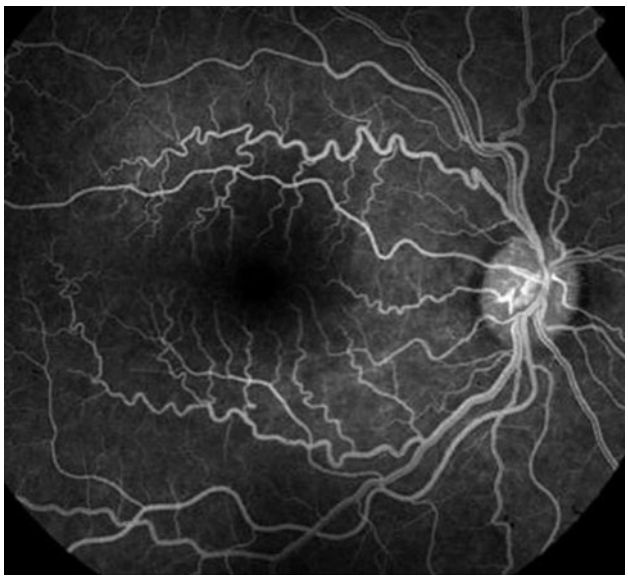

Fig. 7 Retinal fluorescein angiogram from a patient with Fabry's disease showing increased vascular tortuosity with abnormal "corkscrew" vessels. Reproduced from: Fabry disease: Perspectives from 5 years of FOS (2006) with permission from Oxford PharmaGenesis Ltd.

Clearly, the current work has a variety of limitations, including an ad hoc way in which vessel segments were

chosen for analysis. For the purposes of this initial investigation, smoothly curved, regular-appearing, sinusoidal-type vessel segments were chosen for analysis, with the rationale that, if these segments cannot be successfully modeled, then it would be futile to attempt to model the more irregular vessel courses sometimes seen in the body. Certainly, it would be possible to pick other vessels with irregular shapes, kinks, etc., which would show the same deviations from the sine-generated model as do the abnormal retinal vessels analyzed above. Also, there is bound to be some distortion in vessel shape as three-dimensional vessels are rendered as two-dimensional images for the purposes of angiograms, and there is some variability in manually designating the radius of curvature, providing a significant range of variability in possible results. Overall, however, it is hoped that the results of this preliminary work, which provides the first model in the literature attempting to explain physiologic tortuosity in terms of optimal design criteria, serves as a useful starting point for more detailed work, and a springboard for further investigation of tortuosity in health versus disease states, augmenting the pioneering efforts begun by the other groups cited herein.

Appendix A: Deriving the equation of a smooth path of minimal curvature

Consider the x–y plane. Let us say that point C is a point in this plane and that we will connect point O to point C by a smooth path of length L (see Fig. 8). Our goal will be to derive parametric equations that will allow us to describe the path from O to C.

Let us say that point $P(x,y)$ is a point on the path from O to C. The length of the path from O to P will be denoted by l. Additionally, let us define θ to be the angle between the positive direction of the x-axis and the line tangent to the path at point P. Next, we will say that point P′ $(x + \Delta x, y + \Delta y)$ is a point on the path that is close to point P. If the distance between P and P′ is made small enough, it becomes reasonable to use the tangent at point P to approximate the location of P′.

If we say that P and P′ can be connected by a straight line (approximately) then we can say:

$$\frac{\Delta x}{\Delta l} \approx \cos\theta \quad \frac{\Delta y}{\Delta l} \approx \sin\theta$$

where Δl is the O to C in going from P to P′. If we take the limit for $\Delta l \to 0$, then

$$\frac{\mathrm{d}x}{\mathrm{d}l} = \cos\theta \tag{1a}$$

$$\frac{\mathrm{d}y}{\mathrm{d}l} = \sin\theta \tag{1b}$$

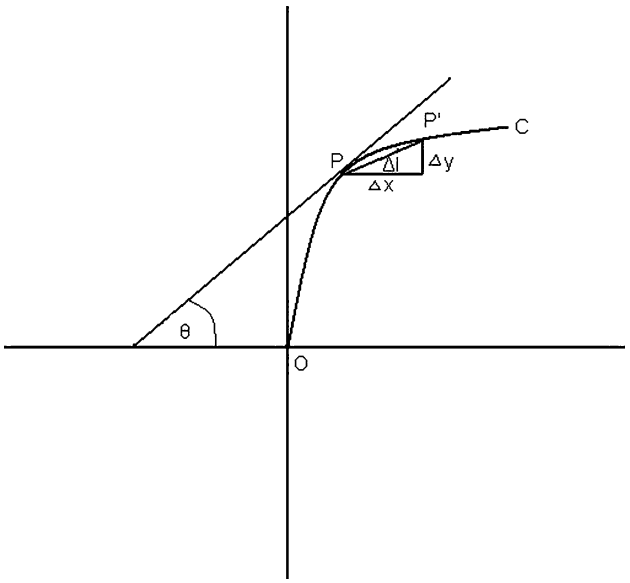

Fig. 8 Region around P showing P′ along with tangent at P

These equations are satisfied by each value l in $0 < l < L$. We can see that, when the value of l changes, the values of x, y, and θ will change in response and so we can think of x, y, and θ as functions of l. The functions $x(l)$ and $y(l)$ describe the position of a point on the curve and $\theta(l)$ describes the direction of the curve at that point.

To find functions for x and y, we can integrate the two above equations with respect to l. This gives us:

$$x(t) = \int_0^t \cos\theta(l)\,\mathrm{d}l \tag{2a}$$

$$y(t) = \int_0^t \sin\theta(l)\,\mathrm{d}l \tag{2b}$$

where t is a variable parameter in the segment $(0,L)$. The above two equations are the parametric equations that describe the path from O to C, where $\theta(l)$ is the direction function of the path.

We will say that the length of the path from O to P is l and that the length of the path from O to P′ is $l + \Delta l$. We can now define the average curvature of the path between P and P′ to be:

$$\frac{\theta(l + \Delta l) - \theta(l)}{\Delta l}$$

If we take the limit of this expression as $\Delta l \to 0$, we can find the curvature at point P. Because the direction angle at any point is a function of l, we can also express the curvature as a function of l. We will denote this function by $c(l)$:

$$c(l) = \lim_{\Delta l \to 0} \frac{\theta(l + \Delta l) - \theta(l)}{\Delta l} = \theta'(l)$$

We can now write that the average curvature, $\bar{c}$, as the integral square average of $\theta'(l)$:

$$\bar{c} = \sqrt{\frac{1}{L}\int_0^L (\theta'(l))^2 \, \mathrm{d}l}$$

This is the continuous analog of the mean square value of n numbers.

Our interest is to find the curve from point O to point C that has the minimum average curvature, assuming a curved path. By examining our expression for $\bar{c}$, and remembering that the square root function always increases along its domain, then we can simplify our problem by noting that we will minimize $\bar{c}$ if we minimize the integral:

$$\int_0^L (\theta'(l))^2 \, \mathrm{d}l \tag{3}$$

Before we can do this, however, we must realize that there are two constraints that must be imposed on the integral above: the x and y coordinates of the path's endpoint C. Attempting to minimize the above integral would allow us to find the minimum curvature for any path of length L. However, we are looking for the minimum average curvature of a path of length L that ends in point C. The constraints can be specified by saying that the coordinates of point C are X_1 and Y_1. Using the parametric equations (Eqs. 2a and 2b) that we developed for the x and y coordinates of any point on the curve, we can say that:

$$X_1 = x(L) = \int_0^L \cos\theta(l) \, \mathrm{d}l$$

$$\mathrm{Y}_1 = y(L) = \int_0^L \sin\theta(l) \, \mathrm{d}l$$

Equivalently,

$$\int_0^L \cos\theta(l) \, \mathrm{d}l - X_1 = 0 \tag{4a}$$

$$\int_0^L \sin\theta(l) \, \mathrm{d}l - Y_1 = 0 \tag{4b}$$

Conceptually, our minimization problem can now be rephrased as the following: minimize Eq. 3 given the functions $\theta(l)$ that are continuous, have a continuous derivative, and satisfy Eqs. 4a and 4b.

We can incorporate the two constraints imposed by the path's endpoint C by using the technique developed by Lagrange. We can begin by writing a new expression that incorporates the integral that we wish to minimize as well as our two constraints:

$$\int_0^L (\theta'(l))^2 \, \mathrm{d}l + \lambda\left(\int_0^L \cos\theta(l) \, \mathrm{d}l - X_1\right) + \mu\left(\int_0^L \sin\theta(l) \, \mathrm{d}l - Y_1\right)$$

which simplifies to

$$\int_0^L \left((\theta'(l))^2 + \lambda\left(\cos\theta(l) - \frac{X_1}{L}\right) + \mu\left(\sin\theta(l) - \frac{Y_1}{L}\right)\right) \mathrm{d}l \tag{5}$$

Appendix B: Solving the differential equation

As was discussed above, our model is based on finding a function $\theta(l)$ that produces a curve from O to C with minimal average curvature. We concluded that such a function, $\theta(l)$, must minimize the integral shown in Eq. 5:

$$\int_0^L \left((\theta'(l))^2 + \lambda\left(\cos\theta(l) - \frac{X_1}{L}\right) + \mu\left(\sin\theta(l) - \frac{Y_1}{L}\right)\right) \mathrm{d}l$$

Using this integral to find the desired function $\theta(l)$ is a problem in the calculus of variations and requires what is known as the Euler–Lagrange equation, which is one of the fundamental theorems of the calculus of variations.

We begin by designating the integrand in Eq. 5 as:

$$F(\theta) = (\theta'(l))^2 + \lambda\left(\cos\theta(l) - \frac{X_1}{L}\right) + \mu\left(\sin\theta(l) - \frac{Y_1}{L}\right)$$

Now let us call F'_θ and $F'_{\theta'}$ the partial derivatives of F with respect to θ and θ' respectively. The Euler–Lagrange equation states that a function $\theta(l)$ that minimizes Eq. 5 will satisfy the following differential equation:

$$F'_\theta = \frac{\mathrm{d}}{\mathrm{d}l}(F'_{\theta'})$$

From the equation for $F(\theta)$, we get that:

$$F'_\theta = -\lambda\sin\theta(l) + \mu\cos\theta(l)$$

$$\frac{\mathrm{d}}{\mathrm{d}l}(F'_{\theta'}) = 2(\theta''(l))$$

By substituting these equations into to Euler equation, we get:

$$2(\theta''(l)) = -\lambda\sin\theta(l) + \mu\cos\theta(l)$$

This gives us a second degree differential equation with $\theta(l)$ being the unknown function.

Ideally, we would now like to solve this differential equation to find the function $\theta(l)$ that will minimize the curvature of the path from point O to point C. However it has been shown to be impossible to find an explicit closed form solution to our differential equation. We can, however, find an approximate solution which, when tested, proves to be quite a good approximation. The derivation of the approximate solution is presented below.

We begin by multiplying the differential equation by $\frac{d\theta}{dl}$:

$$2\frac{d\theta}{dl}(\theta''(l)) = -\lambda\frac{d\theta}{dl}\sin\theta(l) + \mu\frac{d\theta}{dl}\cos\theta(l)$$

By integrating this equation with respect to l, we get:

$$\frac{d}{dl}\left(\frac{d\theta}{dl}\right)^2 = \lambda\frac{d}{dl}(\cos\theta(l)) + \mu\frac{d}{dl}(\sin\theta(l))$$

which can be rewritten as:

$$\frac{d}{dl}\left(\left(\frac{d\theta}{dl}\right)^2 - \lambda\cos\theta(l) - \mu\sin\theta(l)\right) = 0$$

In the above form, we can clearly see that this equation implies that:

$$\left(\frac{d\theta}{dl}\right)^2 - (\lambda\cos\theta(l) + \mu\sin\theta(l)) = C$$

where C is an arbitrary constant.

We now note that the use of a few algebraic manipulations allows us to transform the expression:

$$\lambda\cos\theta(l) + \mu\sin\theta(l)$$

to

$$U\cos(\theta(l) - h) + C$$

where U and h are constants that depend on the values of λ and μ. We can then rewrite the previous equation as:

$$\left(\frac{d\theta}{dl}\right)^2 = U\cos(\theta(l) - h) + C \tag{6}$$

As has been discussed earlier, it is reasonable to assume, based on the shape of the blood vessels as they curve, that $\frac{d\theta}{dl}$ is not a linear function. This implies that the value of U must be non-zero.

Let us also assume that $\theta(l)$ changes in the range:

$$-\omega \le 0 \le \omega$$

where ω is the maximal angle that $\theta(l)$ can reach. We will now choose the value of h to be the average value of $\theta(l)$, and we will assume that this value is 0. This is a reasonable assumption for a blood vessel wave that has an approximate line of symmetry at $l = L/2$. The blood vessels used for this paper have been chosen to assure the validity of this assumption. Now, we will choose the values of C and U such that the following two conditions are met:

1. The right-hand side of Eq. 6 must be non-negative.
2. The solution of Eq. 6 is a periodic function in the variable l. We impose this condition based on consideration of what we already know to be the shape of the blood vessels.

By inspection, we find that we can meet these two conditions by choosing the following values for C and U:

$$U = \alpha^2$$

$$C = -U\cos\omega$$

Plugging the values of h, C, and U into Eq. 6, we get:

$$\frac{d\theta}{dl} = \alpha\sqrt{\cos\theta - \cos\omega}$$

as noted above. This can be rewritten as:

$$\int \frac{d\theta}{\sqrt{\cos\theta - \cos\omega}} = \alpha \times l \tag{7}$$

Equation 7 specifies in an implicit form an infinite set of solutions. As mentioned earlier, it is impossible to find an explicit form for this equation. We can, however, calculate an approximation to the integral which will then allow us to find explicit solutions to the integral. We will start with the trigonometric identity:

$$\cos\theta - \cos\omega = -2\sin\frac{\theta+\omega}{2} \times \sin\frac{\theta-\omega}{2}$$

Let us assume that ω is relatively small. We can then use the approximation that $\sin x \approx x$ which applies for only small values of x. Then, we can say that:

$$\cos\theta - \cos\omega \approx -2\frac{\theta+\omega}{2} \times \frac{\theta-\omega}{2} = \frac{\omega^2 - \theta^2}{2}$$

We can then rewrite Eq. 7 as:

$$\int \frac{d\theta}{\sqrt{\omega^2 - \theta^2}} = \alpha \times l \tag{8}$$

Calculating the integral, we get:

$$\arcsin\frac{\theta}{\omega} = \alpha \times l + \beta$$

where β is an arbitrary constant. Rearranging gives:

$$\theta = \omega\sin(\alpha \times l + \beta) \tag{9}$$

The above equation gives an infinite number of explicit solutions to the differential equation derived using the Euler–Lagrange equation. We now wish to assign values to the constants α and β. In order to do this, we must make

one final assumption. We will assume that the path is tangent to the x-axis at the endpoints of the path (i.e. when $l = 0$ and $l = L$). With this assumption and the equation above, we get:

$$0 = \omega \sin(\alpha \times 0 + \beta) = \omega \sin(\beta) \text{ and thus } \beta = 0$$

Equation 9 then simplifies to:

$$\theta = \omega \sin(\alpha \times l)$$

from which we can say that:

$$0 = \omega \sin(\alpha \times L) \text{ and thus } \alpha = \frac{2\pi}{L}$$

Plugging in this value for α into Eq. 9 gives us the approximate solution to the differential equation derived using the Euler–Lagrange equation:

$$\theta(l) = \omega \sin\left(\frac{2\pi l}{L}\right) \tag{10}$$

where $0 \leq l \leq L$.

The model shows that the sine-generated curve (Eq. 10) is a reasonable and tractable closed-form approximation to the elliptic integrals which represent the curve of minimal average curvature.

References

1. Image from the Department of Ophthalmology and Visual Sciences, University of Iowa Health Care Center. http://webeye.ophth.uiowa.edu/dept/service/photo/fluo1.htm
2. Malamateniou C, Counsell SJ, Allsop JM et al (2006) The effect of preterm birth on neonatal cerebral vasculature studied with magnetic resonance angiography at 3 Tesla. Neuroimage 32(3): 1050–1059
3. Vasu V, Durighel G, Uthaya S et al (2008) Preterm nutrition and cerebral vascular tortuosity at term equivalent age. In: Neonatal Society 2008 Autumn Meeting, London
4. Bullitt E, Rahman FN, Smith JK et al (2009) The effect of exercise on the cerebral vasculature of healthy aged subjects as visualized by MR angiography. AJNR Am J Neuroradiol 30(10): 1857–1863
5. Witt N, Wong T, Hughes A et al (2006) Abnormalities of retinal microvascular structure and risk of mortality from ischemic heart disease and stroke. Hypertension 47:975
6. Bullit E, Zeng D, Gerig G et al (2005) Vessel tortuosity and brain tumor malignancy: a blinded study. Acad Radiol 12:1232–1240
7. Bullitt E, Ewend MG, Aylward S et al (2004) Abnormal vessel tortuosity as a marker of treatment response of malignant gliomas: preliminary report. Technol Cancer Res Treat 3(6):577–584
8. Bullit E, Wolthusen PA, Brubaker L et al (2006) Malignancy-associated vessel tortuosity: a computer-assisted MR angiographic study of choroid plexus carcinoma in genetically engineered mice. Am J Neuroradiol 27:612–619
9. Bullitt E, Lin NU, Smith JK, Zeng D, Winer EP, Carey LA, Lin W, Ewend MG (2007) Blood vessel morphologic changes depicted with MR angiography during treatment of brain metastases: a feasibility study. Radiology 245(3):824–830
10. Bullitt E, Ewend M, Vredenburgh J et al (2009) Computerized assessment of vessel morphological changes during treatment of glioblastoma multiforme: report of a case imaged serially by MRA over four years. Neuroimage 47(Suppl 2):T143–T151
11. Jain R (2001) Normalizing tumor vasculature with anti-angiogenic therapy: a new paradigm for combination therapy. Nat Med 7:987–989
12. Leopold LB, Langbein WB (1966) River meanders. Sci Am 214:60–70
13. Saba L, Mallarini G (2010) Correlation between kinking and coiling of the carotid arteries as assessed using MDCTA with symptoms and degree of stenosis. Clin Radiol 65(9):729–734
14. Bender EA (1978) Basic optimization. The geometry of blood vessels. In: An introduction to mathematical modeling, Chap. 4. Dover, Mineola, pp 71–73
15. Langbein WB, Leopold LB (1966) River Meanders. Theory of minimum variance, US Geological Survey Professional Paper 422-H
16. Movshovitz-Hadar N, Shmukler A (2006) River meandering and a mathematical model of this phenomenon PhysicaPlus, No. 7
17. Von Schelling H (1951) Most frequent particle paths in a plane. Trans Am Geophys Union 32:222–226
18. MacMillan WD (1968) Statics and the dynamics of a particle. Dover, New York, pp 195–201
19. Sodi A, Ioannidis A, Pitz S (2006) Opthalmological manifestations of Fabry disease, image 4. In: Mehta A, Beck M, Sunder-Plassmann G (eds) Fabry disease: perspectives from 5 years of FOS, Chapt. 26. Oxford PharmaGenesis, NCBI National Bookshelf. http://www.ncbi.nlm.nih.gov/books/NBK11599/
20. Beck M (2006) Demographics of FOS- the Fabry outcome survey. In: Mehta A, Beck M, Sunder-Plassmann G (eds) Fabry disease: perspectives from 5 years of FOS, Chap. 16. Oxford PharmaGenesis. NCBI National Bookshelf
21. Sodi A, Ioannidis A, Mehta A et al (2007) Ocular manifestations of Fabry's disease: data from the Fabry Outcome Survey. Br J Ophthalmol 91(2):210–214